Shape-driving effects in the triaxial nucleus, ^{128}Xe

J. N. Orce,[1,2] A. M. Bruce,[1] A. Emmanouilidis,[1] A. P. Byrne,[3,4] G. D. Dracoulis,[3] T. Kibédi,[3] M. Caamaño,[5] H. El-Masri,[5]
C. J. Pearson,[5] Zs. Podolyák,[5] P. D. Stevenson,[5] P. M. Walker,[5] F. R. Xu,[5,6] D. M. Cullen,[7] and C. Wheldon[8,*]

[1]*School of Engineering, University of Brighton, Brighton BN2 4GJ, United Kingdom*
[2]*Department of Physics and Astronomy, University of Kentucky, Lexington, Kentucky 40506-0055, USA*[†]
[3]*Department of Nuclear Physics, Australian National University, Canberra, ACT 0200, Australia*
[4]*Department of Physics, The Faculties, Australian National University, Canberra, ACT 0200, Australia*
[5]*Department of Physics, University of Surrey, Guildford, Surrey GU2 7XH, United Kingdom*
[6]*Department of Technical Physics, Peking University, Beijing 100871, People's Republic of China*
[7]*Department of Physics and Astronomy, University of Manchester, Manchester, M13 9PL, United Kingdom*
[8]*Department of Physics, University of Liverpool, Liverpool L69 7ZE, United Kingdom*
(Received 13 April 2006; published 14 September 2006)

An extended decay scheme for ^{128}Xe has been constructed by using data from the ^{124}Sn(^{9}Be, 5n)^{128}Xe reaction at a beam energy of 58 MeV. Bands have been identified as being built on several intrinsic states, including a proposed 9/2$^-$[514] $\otimes$ 1/2$^+$[400] two-quasineutron configuration that forms the $K^\pi = 5^-$ intrinsic state at 2228 keV, and on a previously assigned $K^\pi = 8^-$ intrinsic state at 2786 keV. A half-life of 73(3) ns has been measured for the latter. Theoretical calculations have been performed by using the configuration-constrained blocking method based on a nonaxial Woods-Saxon potential. Large γ deformation and γ softness are predicted for the ground state and the $K^\pi = 5^-$ intrinsic state, whereas a nearly axially symmetric shape is predicted for the $K^\pi = 8^-$ two-quasiparticle configuration. The low value of the hindrance factor for the $E1$ transition depopulating the $K^\pi = 8^-$ intrinsic state is discussed in the context of analogous transitions in neighbouring $N = 74$ isotones.

I. INTRODUCTION

The nuclide ^{128}Xe is in a region of the nuclear chart that is rich in nuclear structure and provides a testing ground to examine the interplay between triaxial and axially deformed nuclear shapes. A systematic study of the shapes of ground, and neutron and proton s bands across the Xe chain from $A =$ 118 to 130 [1] indicates ground-state deformation changing from prolate in $A = 118$–126 to oblate in $A = 130$, with the neutron s band essentially following the same trend but oblate shapes being favoured for $A > 124$. The proton s band, however, consistently favors a prolate shape. The total Routhian surface calculations [1] for ^{128}Xe are compatible with other interpretations based on the O(6) limit of the interacting boson model [2] in suggesting a triaxial shape for the ground state. This is supported by the observation of the γ band at the relatively low excitation energy of 969 keV [3], indicating the softness of ^{128}Xe with respect to γ excitations and the necessity of including the triaxial degree of freedom in any theoretical approach.

It is therefore somewhat surprising that ^{128}Xe is known to have a $K^\pi = 8^-$ isomeric state [4] with a half-life in the nanosecond region. The K quantum number is defined as the projection of the total angular momentum onto the nuclear symmetry axis and is a good quantum number only

for axially symmetric deformed nuclei. Analogous $K^\pi =$ 8$^-$ isomeric states have been identified in the even-Z, $N = 74$ isotones from $^{130}_{56}$Ba to $^{140}_{66}$Dy [5–11] and are interpreted as being built on the 7/2$^+$[404] $\otimes$ 9/2$^-$[514] two-quasineutron configuration. The systematics of the decay from the $K^\pi = 8^-$ isomeric state to the $J^\pi = 8^+$ member of the yrast band have been discussed [9] for nuclei from ^{130}Ba to ^{138}Gd, but prior to the present work no such transition had been observed for ^{128}Xe. The observation of this transition was therefore one of the experimental goals. Additional motivation was to collect data in this mass region on the "goodness" of the K quantum number in a nucleus that has strong shape-driving effects.

The experimental $E(4^+)/E(2^+)$ ratio, plotted in Fig. 1, shows that ^{128}Xe with $E(4^+)/E(2^+) = 2.33$ lies in the middle of the so-called transitional region, where $E(4^+)/E(2^+) = 2$ for a pure vibrator and 3.33 for a pure rotor. In this case, it is unlikely that the K quantum number will be pure, and the K values listed in this article have therefore been simply assigned as the bandhead spin. In this work we consider the role that triaxiality plays in the validity of K as a good quantum number for different quasiparticle configurations, with particular emphasis on the $K^\pi = 8^-$ isomeric state. The shapes of intrinsic states have been calculated by using the configuration-constrained blocking method [13], and the results are discussed in the context of the decay properties of the intrinsic states and the rotational behavior of bands built on them. The direct decay from the $K^\pi = 8^-$ isomeric state to the 8$^+$ member of the ground-state ($K = 0$) band will be discussed in terms of K mixing in both the initial and the final states.

---

*Current address: SF7, HMI, Glienicker Straße 100, D-14109 Berlin, Germany.

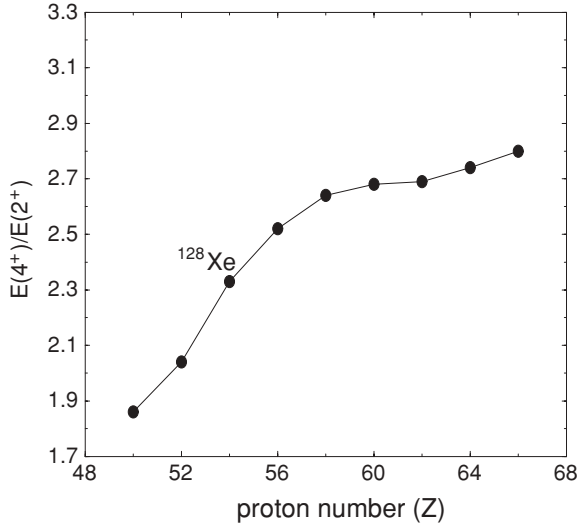†Electronic address: jnorce@pa.uky.edu; URL: http://www.pa.uky.edu/~jnorce

FIG. 1. Experimental $E(4^+)/E(2^+)$ ratio for the even-Z, $N = 74$ isotones as a function of the proton number (data from Refs. [5–9,11, 12] and the current work).

II. EXPERIMENTAL PROCEDURE

High-spin states were populated by using the ^{124}Sn(^{9}Be, $5n$)^{128}Xe fusion-evaporation reaction at a beam energy of 58 MeV. The time profile of the ^{9}Be beam, provided by the 14UD Pelletron Tandem accelerator at the Australian National University, was ∼1 ns pulses separated by 1.7 μs. These pulses were incident on a 3 mg/cm^2 thick ^{124}Sn target which stopped most of the recoiling nuclei.

Time correlated γ-ray events were collected by using the CAESAR array [14], comprising six Compton suppressed n-type coaxial HPGe detectors placed at (θ, ϕ) angles of (48°, 0°), (48°, 180°), (97°, 0°), (97°, 180°), (145°, 0°), and (145°, 180°) where the z axis is along the beam and the x axis ($\phi = 0°$) is vertically upward. Two small volume unsuppressed planar germanium detectors (LEPS) were placed at (45°, 270°) and (135°, 270°). There were two different experiments:

(i) A singles measurement in which the energies of γ rays and their arrival time relative to the beam bunch were measured,

(ii) A coincidence measurement in which the energies of a pair of γ rays observed within ±856 ns were recorded along with their time, measured with respect to the rf pulse train.

Data were written to disk for subsequent off-line analysis, where they were sorted [15] into a variety of matrices and cubes. The Radware analysis software package [16] and the ANA program [17] were used to analyze the data. Data from the singles experiment was used to construct two time-energy matrices that contained the γ-ray energy on one axis and the time of arrival of the γ ray on the other. One matrix contained data from the germanium detectors, and the other data from the LEPS detectors. In the coincidence experiment only data from the germanium detectors were used to construct energy-energy-time cubes and the following matrices: (i) a

γ-γ-coincidence matrix, where the γ rays were observed within a time difference of up to ±43 ns, (ii) an early-delayed γ-γ matrix containing events that have a time difference between 44 and 784 ns, (iii) an out-of-beam matrix using events that have a time difference of up to ±43 ns and that were measured between 50 and 1590 ns after the arrival of the beam pulse, and (iv) a directional correlations from oriented state (DCO) matrix, where the two axes correspond to γ rays observed in the detectors placed at $\theta = 48°$ and $\theta = 97°$.

Where possible, the multipolarity of a γ-ray transition was obtained by using the DCO [18] method. Although some of the initial alignment can be lost following decay from an isomeric state, in the case of short (nanosecond) isomeric lifetimes useful conclusions can still be drawn from consideration of the DCO ratios. The experimental DCO ratio, R_{DCO}, is defined here as

$$R_{\text{DCO}} = \frac{I_{\gamma_1}(48°) \text{ gated by } \gamma_2(97°)}{I_{\gamma_1}(97°) \text{ gated by } \gamma_2(48°)}. \qquad (1)$$

DCO ratios were obtained by gating only on stretched quadrupole transitions below the transition of interest. $\Delta J = 2$ and pure ($\delta = 0$) $\Delta J = 1$ transitions are expected to have R_{DCO} values of 1 and ∼0.56, respectively. Mixed $M1/E2$ transitions can have an R_{DCO} value between 0.3 and 1.2, depending on ΔJ and the sign and size of the mixing ratio δ.

III. EXPERIMENTAL RESULTS

The total projection of the γ-γ-coincidence matrix confirms ^{128}Xe as the main channel in the reaction with over 50% of the total cross section. The ^{128}Xe level scheme built in the present work is shown in Fig. 2, and Table I lists the relative intensities of γ-ray transitions. The intensities have been measured in the total projection of the γ-γ-coincidence matrix. Since this matrix includes data at the three detector angles, it can be considered to average out some of the angular distribution effect and therefore gives a measure of the relative intensities of the transitions. In cases where transitions are too weak to be observed in this matrix or are considered to be contaminated, their intensity has been obtained from intensity balances in coincidence spectra. Column 5 of table I includes the measured R_{DCO} values, which for previously known [3,4,19] $\Delta J = 2$ (590, 704, 775, 684, and 612 keV) and pure ($\delta = 0$) $\Delta J = 1$ (303, 504, 846, and 1196 keV) transitions, respectively, average 1.01(2) and 0.56(2), in agreement with the expected values of 1 and ∼0.56. The results for previously known transitions are in good agreement with earlier work [3,4,19].

A. Ground-state and s bands

Prior to this experiment the highest angular momentum observed in ^{128}Xe was associated with the proposed 16$\hbar$ state at 5570 keV [19]. In the current work, this is confirmed with a measured R_{DCO} value of 0.89(7) for the 954 keV depopulating transition. Figure 3 shows a γ-ray spectrum gated by the $14^+ \rightarrow 12^+$, 808 keV transition in the γ-γ-coincidence matrix. Gamma-rays of energies 1033, 1105, and 1182 keV have

TABLE I. Levels and transitions obtained from the ^{124}Sn(^{9}Be, $5n$)^{128}Xe reaction at a beam energy of 58 MeV. I_γ denotes the efficiency corrected relative intensities resulting from the analysis of the γ-γ coincidence matrix. The intensity of the 443 keV γ-ray transition ($2^+ \rightarrow 0^+$) has been normalized to 1000 units. An asterisk (*) indicates that the intensities are estimated from coincidence gates. R_{DCO} denotes the DCO ratios measured by gating below on stretched $E2$ transitions.

E_γ	E_i	E_f	I_γ	R_{DCO}	J_i^π	J_f^π
159.2(5)	5816.7	5657.4	4(1)*			
204.0(3)	2786.3	2582.3	12(1)*	0.76(4)	8^-	7^-
204.8(4)	3412.0	3207.2	15(2)*		(9^-)	9^-
271.4(4)	2499.8	2228.4	49(3)	0.65(2)	6^-	5^-
273.1(5)	3214.1	2941.0	18(2)	0.47(3)	(9^+)	(8^+)
274.4(4)	2786.3	2511.9	0.08(4)*		8^-	8^+
279.0(5)	4086.6	3807.6	32(1)	0.64(5)	(12^+)	12^+
286.5(3)	2786.3	2499.8	21(1)	1.13(7)	8^-	6^-
290.5(5)	3883.0	3592.5	4(1)		11^-	10^-
297.7(4)	3412.0	3114.3	16(1)	1.18(21)	(9^-)	9^-
302.2(4)	2582.3	2280.1	13(1)	0.78(20)	7^-	6^+
319.8(5)	4868.0	4548.2	27(3)	0.65(6)	(14^+)	(13^+)
328.0(5)	3114.3	2786.3	28(2)	0.37(2)	9^-	8^-
344.7(4)	5678.5	5334.1	7(1)*		(16^+)	(15^+)
353.8(4)	2582.3	2228.4	44(2)	1.23(9)	7^-	5^-
392.9(4)	1995.7	1602.9	2(1)*		5^+	4^+
396.0(4)	1428.7	1032.7	2(1)*		3^+	4^+
396.3(4)	6074.8	5678.5	13(2)*		(17^+)	(16^+)
417.5(5)	4909.8	4492.2	9(2)*		13^-	(12^-)
420.8(5)	3207.2	2786.3	8(1)	0.62(9)	9^-	8^-
429.1(3)	2941.0	2511.9	35(2)	1.17(9)	(8^+)	8^+
438.8(4)	3412.0	2973.1	18(2)	0.51(5)	(9^-)	8^+
442.6(3)	442.6	0.0	1000(6)		2^+	0^+
459.6(3)	1428.7	969.0	9(1)*		3^+	2^+
461.2(3)	2973.1	2511.9	15(2)*	0.87(6)	8^+	8^+
461.6(5)	4548.2	4086.6	40(5)*		(13^+)	(12^+)
466.1(5)	5334.1	4868.0	13(2)*		(15^+)	(14^+)
467.2(3)	3049.4	2582.3	13(2)		8^-	7^-
474.1(4)	4066.6	3592.5	3(2)*	0.61(20)	(11^-)	10^-
478.2(4)	3592.5	3114.3	27(2)	0.42(6)	10^-	9^-
484.8(4)	4077.3	3592.5	27(1)	0.47(9)	11^-	10^-
490.2(3)	2718.6	2228.4	10(2)*			5^-
491.8(4)	2228.4	1736.5	3(1)*		5^-	6^+
504.1(3)	2499.8	1995.7	20(2)	0.73(5)	6^-	5^+
526.4(3)	969.0	442.6	18(2)		2^+	2^+
532.0(4)	3114.3	2582.3	53(2)	0.89(6)	9^-	7^-
543.6(4)	2280.1	1736.5	21(2)	0.63(7)	6^+	6^+
549.6(3)	3049.4	2499.8	55(3)	0.90(6)	8^-	6^-
550.1(5)	5459.9	4909.8	13(4)*	0.53(5)	(14^-)	13^-
567.0(4)	1995.7	1428.7	12(1)*		5^+	3^+
569.3(5)	7015.5	6446.2	15(2)*			
570.2(4)	1602.9	1032.7	9(3)		4^+	4^+
590.1(3)	1032.7	442.6	846(6)	1.06(5)	4^+	2^+
609.3(4)	4492.2	3883.0	6(1)*		(12^-)	11^-
612.2(3)	3807.6	3195.5	272(3)	0.97(4)	12^+	10^+
624.9(4)	3207.2	2582.3	50(3)	0.98(7)	9^-	7^-
625.5(4)	2228.4	1602.9	13(1)*		5^-	4^+
629.5(4)	6446.2	5816.7	9(1)*			
633.9(4)	1602.9	969.0	9(3)		4^+	2^+
654.6(4)	4066.6	3412.0	74(5)	0.91(9)	(11^-)	(9^-)
656.1(4)	3705.5	3049.4	42(5)	0.88(4)	10^-	8^-
670.0(4)	5285.9	4615.9	10(2)*	0.88(14)	(16^+)	14^+

TABLE I. (*Continued.*)

| E_γ	E_i	E_f	I_γ	R_{DCO}	J_i^π	J_f^π
675.8(4)	3883.0	3207.2	19(2)	0.78(8)	11^-	9^-
677.7(4)	2280.1	1602.9	2(1)		6^+	4^+
683.6(5)	3195.5	2511.9	332(3)	0.98(4)	10^+	8^+
693.0(5)	2973.1	2280.1	4(2)		8^+	6^+
703.8(3)	1736.5	1032.7	613(5)	1.06(5)	6^+	4^+
709.1(5)	5459.9	4750.8	7(2)*	0.83(7)	(14^-)	13^-
737.2(5)	4803.8	4066.6	64(6)*	0.92(9)	(13^-)	(11^-)
737.6(4)	4443.1	3705.5	33(6)*	0.96(5)	12^-	10^-
768.3(4)	2499.8	1736.5	10(1)		6^-	6^+
768.8(4)	3883.0	3114.3	52(2)	1.00(9)	11^-	9^-
775.4(3)	2511.9	1736.5	444(4)	1.01(5)	8^+	6^+
781.3(5)	4868.0	4086.6	30(4)*		(14^+)	(12^+)
787.6(4)	5230.7	4443.1	37(7)*	0.89(6)	14^-	12^-
788.0(4)	6247.9	5459.9	27(8)*	0.96(9)	(16^-)	(14^-)
788.8(4)	6446.2	5657.4	42(3)*			
794.3(5)	3989.8	3195.5	12(1)	0.38(5)	(11^+)	10^+
806.1(4)	3592.5	2786.3	12(2)*	0.94(7)	10^-	8^-
808.3(4)	4615.9	3807.6	137(3)	0.98(6)	14^+	12^+
810.5(5)	5678.5	4868.0	23(3)*		(16^+)	(14^+)
817.4(5)	4807.3	3989.8	8(1)*	1.15(19)	(13^+)	(11^+)
832.5(5)	4909.8	4077.3	20(2)*	1.13(12)	13^-	11^-
845.9(3)	2582.3	1736.5	140(3)	0.51(3)	7^-	6^+
846.0(4)	5096.0	4250.0	10(2)*	0.95(9)	14^+	12^+
851.7(4)	3363.6	2511.9	62(5)*	0.99(6)	10^+	8^+
853.6(4)	5657.4	4803.8	64(5)*	0.99(9)	(15^-)	(13^-)
859.4(4)	4066.6	3207.2	7(2)*	1.25(13)	(11^-)	9^-
867.8(5)	4750.8	3883.0	39(5)	0.93(9)	13^-	11^-
870.1(4)	4077.3	3207.2	47(5)*	0.84(7)	11^-	9^-
870.7(4)	5966.7	5096.0	11(2)*	1.23(12)	16^+	14^+
874.1(5)	5490.0	4615.9	24(1)	0.48(5)	(15^+)	14^+
885.2(5)	6115.9	5230.7	9(2)*	0.78(7)	16^-	14^-
886.4(4)	4250.0	3363.6	43(2)*	1.08(9)	12^+	10^+
898.8(5)	6184.7	5285.9	8(2)*		(18^+)	(16^+)
899.8(4)	4492.2	3592.5	7(2)*		(12^-)	10^-
906.1(5)	5713.4	4807.3	11(1)*	0.86(14)		(13^+)
933.1(3)	6645.2	5712.2	9(1)*		(17^-)	15^-
936.5(3)	6648.7	5712.2	9(1)*		(17^-)	15^-
939.6(4)	7014.4	6074.8	14(2)*		(19^+)	(17^+)
954.3(4)	5570.2	4615.9	90(1)	0.89(7)	16^+	14^+
961.4(5)	5712.2	4750.8	18(1)*	0.80(9)	15^-	13^-
963.0(4)	1995.7	1032.7	6(1)*		5^+	4^+
969.0(4)	969.0	0.0	5(1)		2^+	0^+
979.9(3)	7227.8	6247.9	18(1)	1.38(25)	(18^-)	(16^-)
986.1(4)	1428.7	442.6	6(1)*		3^+	2^+
994.6(4)	8009.0	7014.4	6(1)*	1.27(20)	(21^+)	(19^+)
999.6(5)	4807.3	3807.6	13(1)*	0.49(6)	(13^+)	12^+
1026.8(5)	4909.8	3883.0	7(1)*	0.82(9)	13^-	11^-
1032.9(3)	6603.1	5570.2	33(1)	0.87(9)	18^+	16^+
1069.9(5)	7254.6	6184.7	3(1)*		(20^+)	(18^+)
1104.9(3)	7708.0	6603.1	20(1)	1.43(37)	20^+	18^+
1182.0(3)	8889.9	7708.0	5(1)	0.91(9)	22^+	20^+
1195.7(3)	2228.4	1032.7	85(2)	0.55(4)	5^-	4^+
1236.9(4)	8944.9	7708.0	5(1)		(22^+)	20^+
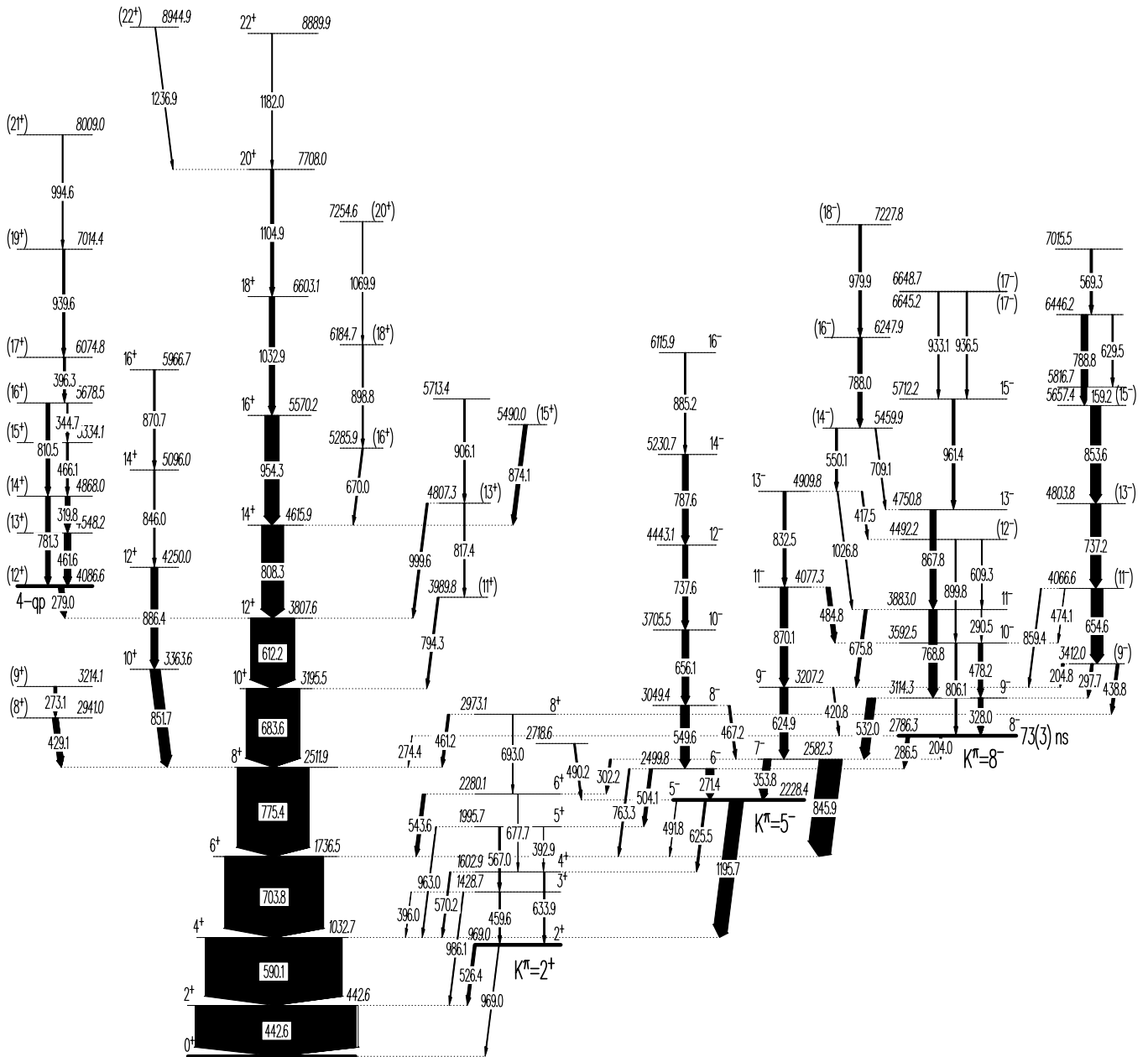
FIG. 2. Level scheme for ^{128}Xe constructed in the present work. The γ-ray energies are given in keV, and the thickness of the arrows represents the relative γ-ray intensity.

been assigned as the extension of the yrast band to $22\hbar$ (see Fig. 2). The measured R_{DCO} values for these decays of 0.87(9), 1.43(37), and 0.91(9), respectively, support their assignments as $\Delta J = 2$ transitions. The 1237 keV transition has been placed as feeding the $J^\pi = 20^+$ level, since it is not observed in coincidence with the 1182 keV transition.

A $J^\pi = 10^+$ state at 3364 keV feeding the 8^+ member of the yrast band was proposed by Lönnroth *et al.* [19]. The current work has identified a band built on this state, which has been extended to a proposed $J^\pi = 16^+$ state at 5967 keV. These states are considered to be part of the ground-state band, while the yrast states above $J^\pi = 8^+$ are members of the rotation-aligned s band.

B. $K^\pi = 2^+$ band

The $K^\pi = 2^+$ γ band built on the 969 keV state was proposed up to the $J^\pi = 6^+$ level by Neuneyer *et al.* [3]. It has been observed in the current experiment and an extension to the $J^\pi = 8^+$ state at 2973 keV is proposed. The 2973 keV state has been observed previously [3,4,20], but no J^π value has been assigned to it. It decays via a 461 keV transition to the $J^\pi = 8^+$ member of the ground-state band and a 693 keV transition [3] to the $J^\pi = 6^+$ member of the $K^\pi = 2^+$ band. Neuneyer *et al.* [3] measured the a_2 and a_4 coefficients for the 461 keV transition but were not able to conclude anything from the values. In the current work the R_{DCO} value for the 461 keV transition has been measured as 0.87(6), and this is consistent
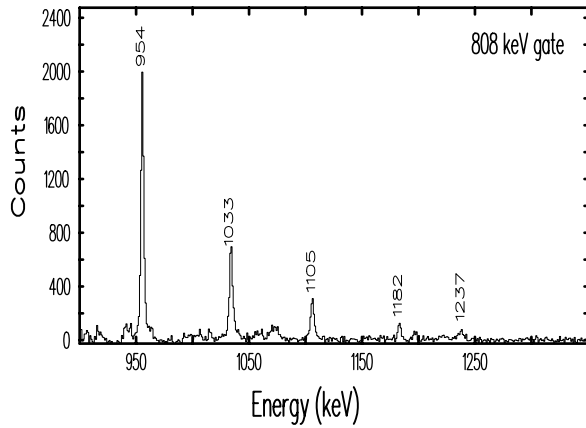
FIG. 3. Gamma-ray spectrum produced by gating on the 808 keV transition in the γ-γ-coincidence matrix.

with a $J \rightarrow J$ transition. Hence a J^π value of 8^+ has been assigned. The level is assumed to be part of the $K^\pi = 2^+$ band because of the level energy systematics and the decay to the $J^\pi = 6^+$ member of the $K^\pi = 2^+$ band.

C. $J^\pi = 5^-$ state at 2228 keV

The measurement of the DCO ratio for the 1196 keV transition depopulating the state at 2228 keV as $R_{\mathrm{DCO}} = 0.55(4)$ is in agreement with the $J^\pi = 5^-$ assignment proposed in previous work [4,19]. Figure 4(a) shows a spectrum gated by the 1196 keV transition in the γ-γ-coincidence matrix, where transitions that form a band above the $J^\pi = 5^-$ state

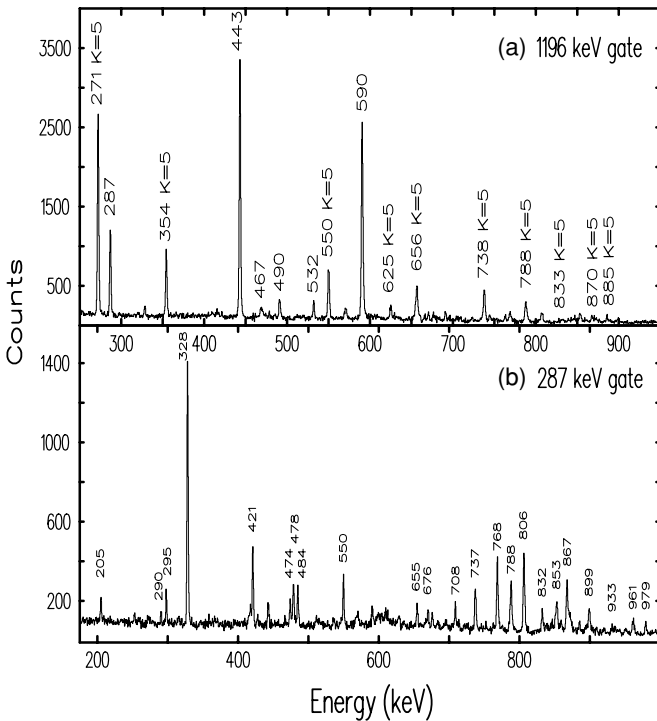FIG. 4. Gamma-ray spectra produced by gating on (a) the 1196 keV transition in the γ-γ-coincidence matrix and (b) the 287 keV transition in the early-delayed matrix.
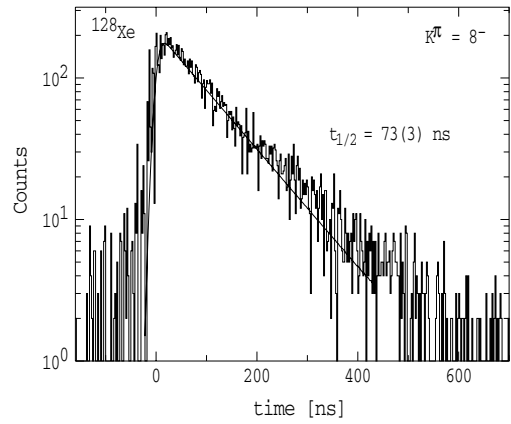

FIG. 5. Time spectrum obtained by gating on the 287 and 328 keV and on the 204 and 328 keV transitions in the γ-γ-time cube. The solid curve shows the best fit including a prompt Gaussian response function and a single exponential decay.

are identified. No lifetime longer than 5 ns has been measured for this state.

D. $K^\pi = 8^-$ intrinsic state at 2786 keV

The intrinsic state at 2786 keV was previously assigned as $J^\pi = K^\pi = 8^-$ following a measurement of the g factor by Lönnroth *et al.* [19]. Figure 4(b) shows a spectrum gated by the delayed 287 keV depopulating transition in the early-delayed matrix, where a complex band structure is identified (see Fig. 2). The decay paths have been linked on the basis of the analysis of the γ-γ-coincidence matrix.

Figure 5 shows the time spectrum obtained by gating on the 287 and 328 keV and on 204 and 328 keV transitions in the γ-γ-time cube. The individual time spectra showed the same exponential decay and hence were summed to improve the statistics. The best fit to the combined spectrum using the convolution of a Gaussian prompt response function and a single exponential decay gives a half-life of $t_{1/2} = 73(3)$ ns, as shown in Fig. 5. This result is in good agreement with a previous half-life measurement of $t_{1/2} = 63(12)$ ns performed by Goettig *et al.* [4] and in disagreement with Lönnroth *et al.* [19], who reported $t_{1/2} = 83(2)$ ns. Figure 6 shows a spectrum
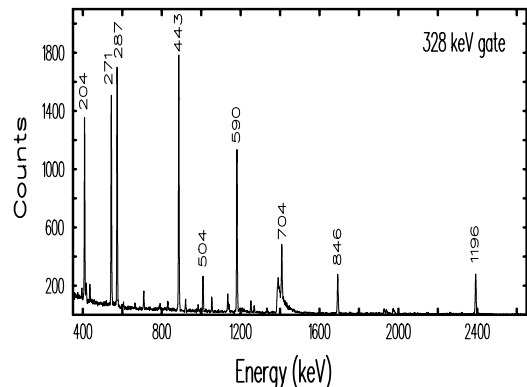

FIG. 6. Gamma-ray spectrum produced by gating on the 328 keV transition in the early-delayed matrix.
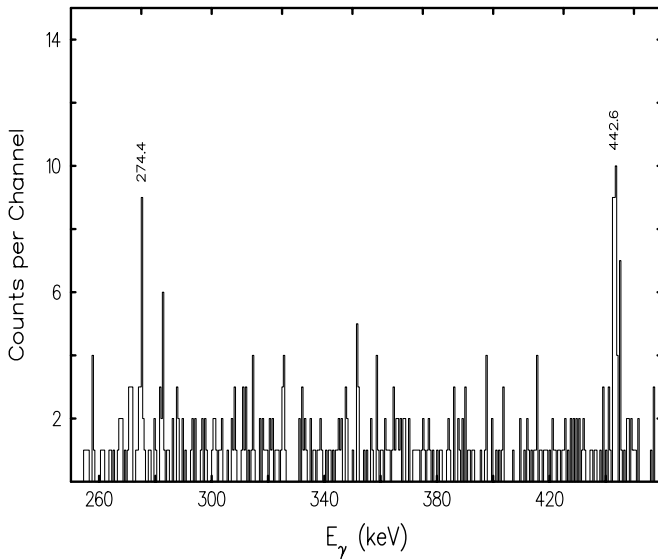
FIG. 7. Gamma-ray spectra gated by the 775 keV transition in the out-of-beam matrix.

of delayed γ rays gated on the $9^- \rightarrow 8^-$, 328 keV transition in the early-delayed matrix.

Transitions observed below the $K^\pi = 8^-$ isomeric state are consistent with previous work [4,19]. In addition, the direct decay from the $K^\pi = 8^-$ isomeric state to the $J^\pi = 8^+$ member of the yrast band proceeds via a 274 keV transition. This transition is very weak, and Fig. 7 shows a gate on the 775 keV transition that depopulates the yrast $J^\pi = 8^+$ state. The figure shows evidence for both the 274 and the 443 keV $(2^+ \rightarrow 0^+)$ transitions, and other portions of the spectrum show evidence of the $4^+ \rightarrow 2^+$ and $6^+ \rightarrow 4^+$ transitions. The intensity of the 274 keV transition, quoted in Table I, has been obtained from this spectrum.

The decay from the $K^\pi = 8^-$ isomeric state also proceeds via 287 and 204 keV transitions to states of $J^\pi = 6^-$ and 7^- respectively. The 287 keV transition is a stretched $E2$ transition, and the 204 keV transition is of mixed $M1/E2$ character.

E. $J^\pi = 9^-$ state at 3412 keV

This level is proposed on the basis of three depopulating transitions (205 and 298 keV to $J^\pi = 9^-$ states and 439 keV to the $J^\pi = 8^+$ state at 2973 keV). All three transitions have about the same intensity, and R_{DCO} values of 1.18(21) and 0.51(5) have been measured for the latter two. The last value is consistent with the 439 keV transition's being a pure $(\delta = 0)$ $\Delta J = 1$ transition. The value for the 298 keV transition is consistent with that expected for a $J \rightarrow J$ transition, so a J^π value of 9^- is proposed for the 3412 keV level. Values of R_{DCO} for the 655, 737, and 854 keV transitions of 0.91(9), 0.92(9), and 0.99(9), respectively, are consistent with $\Delta J = 2$ transitions so a rotational structure above the $J^\pi = 9^-$ state is proposed. The assignment of $J^\pi = 9^-$ for the 3412 keV state is further strengthened by the 859 keV transition from the 4067 keV state to the 3207 keV ($J^\pi = 9^-$) state having

an R_{DCO} value of 1.25(13). This is consistent with a $\Delta J = 2$ transition.

F. $J^\pi = 12^+$ state at 4087 keV

A new structure is proposed based on the 4087 keV level. The R_{DCO} ratio for the 279 keV transition depopulating this level and feeding the yrast 12^+ level is 0.64(5). This is consistent with either a $J \rightarrow J - 1$ dipole or a mixed $J \rightarrow J$ transition, indicating possible J^π values of $12^\pm$ or $13^\pm$. Since the $J \rightarrow J$ transition must be mixed, this indicates an $M1/E2$ transition rather than $E1/M2$, and hence the $J^\pi = 12^-$ possibility is discarded. If the level has $J^\pi = 12^+$, and since the 279 keV transition contains some $E2$ component, some competition from the $E2$ decay to the yrast 10^+ state would be expected (via an 891 keV transition). No such transition is observed. If, however, a $J^\pi = 13^\pm$ assignment is made, the level sequence is yrast and would be expected to be more strongly populated. On weighing up the arguments, the $J^\pi = 12^+$ assignment is preferred. Of the transitions observed within the band structure, the only one where it has been possible to measure a R_{DCO} ratio is the 320 keV transition [$R_{DCO} = 0.65(6)$], and this is consistent with a $\Delta J = 1$ transition. Examination of time spectra produced by gating on transitions above and below the 4087 keV level lead to an upper limit of 5 ns for the half-life of this state.

IV. DISCUSSION

A. Shape driving effects due to two-quasiparticle configurations

The configuration-constrained blocking method, developed by Xu *et al.* [13], has been chosen on account of its successful application to the region of interest [21]. It is based on a nonaxial Woods-Saxon potential and treats β and γ as dynamical variables. In order to obtain the configuration-dependent potential energy surface (PES) for a given multi-quasiparticle state, a process of adiabatic blocking is necessary, whereby the given orbits that are occupied by the specified quasiparticles are followed and blocked. In an axially symmetric Woods-Saxon potential, the single-particle states may be specified by the Ω quantum number (the spin projection onto the symmetry axis). However, for nonaxial shapes, Ω is not conserved. Indeed, the only symmetries still preserved are reflection symmetry (implying conserved parity) and a rotation by $180°$ about the x axis (the signature quantum number α). For even-mass nuclei $\alpha = 0$ or 1, and for odd-mass nuclei $\alpha = \pm 1/2$. Since the quantum number Ω is no longer good, a way to follow a given configuration must be given. The model calculates a set of average Nilsson numbers, $\langle N \rangle$, $\langle n_z \rangle$, $\langle \Lambda \rangle$ and $\langle |\Omega| \rangle$ for the configurations to be constrained in the deformation space. For most of the orbits involved in the multi-quasiparticle configurations in the mass $A \sim 130$ region, these average numbers are well defined and quite stable over the deformation area considered. The nuclear shape is finally obtained by minimizing the calculated potential energy in the quadrupole (β_2, γ) plane, with hexadecapole (β_4) variation.

TABLE II. Calculated shapes and excitation energies E_{cal} (MeV) using the configuration-constrained blocking method for the ground-state and two-quasiparticle configurations in ^{128}Xe. These are compared with the experimentally determined values, E_{exp}.

K^{π}	E_{exp}	E_{cal}	Configuration	β_2	$|\gamma|$	β_4
0^+	0.0	0.0	ground-state	0.134	32.4°	0.000
5^-	2.23	2.17	$9/2^-[514]\otimes1/2^+[400]$	0.142	35.4°	−0.004
8^-	2.78	2.49	$9/2^-[514]\otimes7/2^+[404]$	0.160	6.1°	−0.008

Figure 8 and Table II show the calculated PESs and excitation energies for different two-quasiparticle configurations. The results for the ground and $J^{\pi} = 8^-$ states are consistent with those published in Xu *et al.* [21]. The upper panel of Fig. 8 shows the PES calculation performed for the ground-state (zero rotation, $\hbar\omega = 0$). A triaxial shape is predicted with $|\gamma| = 32.4°$, $\beta_2 = 0.134$, and $\beta_4 = 0.000$. This figure also shows that the ground state is predicted to be soft against the γ degree of freedom.

A $9/2^-[514] \otimes 1/2^+[400]$ two-quasiparticle configuration is proposed for the $K^{\pi} = 5^-$ state, with a predicted excitation energy of 2.17 MeV. This value is in good agreement with the experimentally determined energy ($E_{exp} = 2.23$ MeV) and with previous work [22], where an equivalent $\nu(1h_{11/2}^{-1}3s_{1/2}^{-1})$ two-hole configuration with a calculated energy of $\sim$2.4 MeV was proposed for this state. The middle panel of Fig. 8 shows the results of the PES calculation for the $K^{\pi} = 5^-$ configuration, which is predicted (at $\hbar\omega = 0$) to have a triaxial shape with $|\gamma| = 35.4°$, $\beta_2 = 0.142$, and $\beta_4 = -0.004$. Similar negative-parity bands have been observed in the $N = 72$ isotone ^{126}Xe [23], where large signature splitting between the members of the two signature bands was associated with triaxial deformation. However, the corresponding bands in ^{128}Ba [24] show no signature splitting, and this might be due to a triaxial deformation that decreases as β_2 increases. This is consistent with previous work on the odd-even Ba, Ce, Nd, and Sm isotopes ($A \sim 130$), which associates triaxiality with large signature splittings, the latter being larger as Z and β_2 decrease [25] and the closed shell $Z = 50$ is approached. In principle, it is possible that the $K^{\pi} = 5^-$ band could contain octupole admixtures, which would cause a lower spin for the (unobserved) band head, and a corresponding decrease in the K value associated with the band. Such behavior has been observed in the Os and Hf isotopes [26,27], where it has been proposed that the low-lying octupole vibration is crossed at moderate frequency by a shape-driving, two-quasiproton excitation. In fact, a $J^{\pi} = 3^-$ state has been proposed in ^{128}Xe [3] at an excitation energy of 2138.6 keV, but it is not observed in the current work. This is not surprising, since a heavy-ion reaction that populates only near-yrast states has been used. However, if the observed band were based on an octupole configuration, it would be expected that the energy difference between the $J^{\pi} = 7^-$ and 5^- states would mimic that between the yrast 4^+ and 2^+ states [28,29] and be about 590 keV. Since the observed value is 353 keV, this provides further evidence for the $J^{\pi} = 5^-$ levels being an intrinsic state.

The bottom panel of Fig. 8 shows that the $K^{\pi} = 8^- 7/2^+[404] \otimes 9/2^-[514]$ configuration is expected to have a nearly axially symmetric shape with $|\gamma| = 6°$, $\beta_2 = 0.160$ and $\beta_4 = -0.008$ ($\hbar\omega = 0$). In addition, the excitation energy of the $K^{\pi} = 8^-$ state is predicted at 2.49 MeV, in reasonable agreement with the experimentally determined value of 2.78 MeV. The symmetric deformation predicted for the $K^{\pi} = 8^-$ configuration implies that K might still be a good quantum number in this case.

B. Four-quasiparticle configurations

Table III lists the low-lying four-quasiparticle configurations for this nucleus, calculated by using the same method as

TABLE III. $4qp$ states calculated in ^{128}Xe.

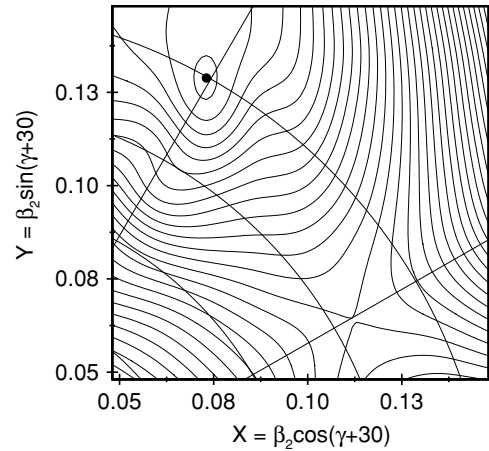| K^{π}	Configuration	β_2	$|\gamma|$	β_4	E(MeV)
12^+	$\nu\{7/2^-[523] \otimes 7/2^+[404] \otimes 9/2^-[514] \otimes 1/2^+[400]\}$	0.154	30°	0.076	4.48
10^-	$\nu\{7/2^+[404] \otimes 9/2^-[514]\} \otimes \pi\{1/2^+[420] \otimes 3/2^+[422]\}$	0.170	0°	−0.014	4.75
13^+	$\nu\{7/2^-[523] \otimes 7/2^+[404] \otimes 9/2^-[514] \otimes 3/2^+[402]\}$	0.152	0°	−0.005	4.95
9^-	$\nu\{7/2^+[404] \otimes 9/2^-[514]\} \otimes \pi\{1/2^+[430] \otimes 1/2^+[420]\}$	0.157	0°	−0.023	5.17
14^+	$\nu\{7/2^-[523] \otimes 9/2^-[514] \otimes 5/2^+[402] \otimes 7/2^+[404]\}$	0.165	32°	0.008	5.42
10^-	$\nu\{7/2^+[404] \otimes 9/2^-[514]\} \otimes \pi\{1/2^+[420] \otimes 3/2^+[411]\}$	0.163	23°	−0.006	5.54
11^-	$\nu\{7/2^+[404] \otimes 9/2^-[514]\} \otimes \pi\{3/2^+[422] \otimes 3/2^+[411]\}$	0.153	0°	−0.023	5.66
12^-	$\nu\{5/2^+[402] \otimes 7/2^+[404] \otimes 9/2^+[514] \otimes 3/2^+[402]\}$	0.152	0°	0.004	5.68
13^-	$\nu\{7/2^+[404] \otimes 9/2^-[514]\} \otimes \pi\{9/2^+[404] \otimes 1/2^+[420]\}$	0.205	0°	−0.024	5.84
13^-	$\nu\{7/2^+[404] \otimes 9/2^-[514]\} \otimes \pi\{9/2^+[404] \otimes 1/2^+[430]\}$	0.197	0°	−0.042	6.50
12^-	$\nu\{7/2^+[404] \otimes 9/2^-[514]\} \otimes \pi\{5/2^+[413] \otimes 3/2^+[411]\}$	0.126	0°	−0.035	6.66
12^-	$\nu\{9/2^-[514] \otimes 1/2^+[400]\} \otimes \pi\{9/2^+[404] \otimes 5/2^+[413]\}$	0.177	15°	−0.019	7.15

FIG. 9. Potential energy surface for the $J^\pi = 12^+$ state at 4.48 MeV. The energy difference between the contours is 50 keV.

therefore nominal, but the four-quasiparticle nature is well defined, and the energy is an upper bound, since projection of pure K states will include at least one state below the 4.48 MeV triaxial configuration. The potential energy surface for this configuration is shown in Fig. 9. Table III shows that the lowest $J^\pi = 13^-$ state is calculated at 5.84 MeV with the lowest $J^\pi = 13^+$ state at 4.95 MeV, both considerably above the experimental energy of 4.09 MeV.

C. Decay of the $K^\pi = 8^-$ state

Figure 10 shows the excitation energy of the $K^\pi = 5^-$, $J^\pi = 7^-$, and $K^\pi = 8^-$ negative parity states and the $J^\pi = 8^+$ member of the yrast band along the even-Z, $N = 74$ isotones. As the $Z = 50$ closed shell is approached, the $N = 74$ isotones
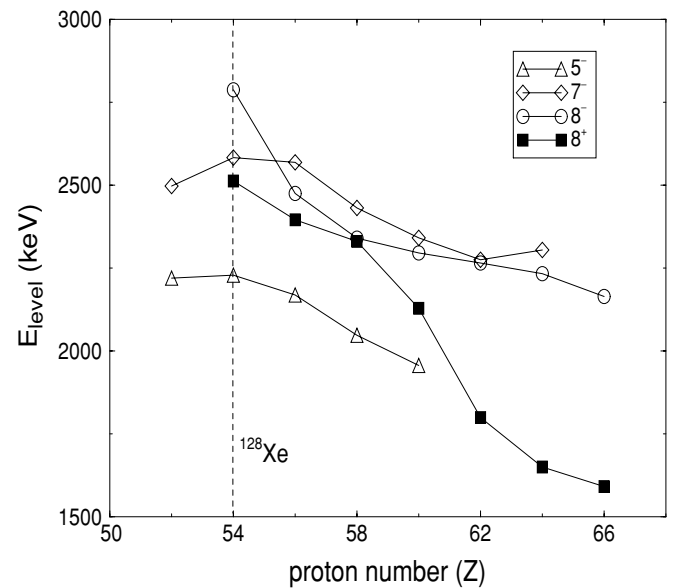

FIG. 10. Excitation energies of the $J^\pi = 5^-, 7^-$, 8^-, and 8_1^+ states in the even-Z, $N = 74$ isotones as a function of the proton number.

FIG. 8. PES calculations for (top) the ^{128}Xe ground state; (middle) $K^\pi = 5^-$, and (bottom) $K^\pi = 8^-$ intrinsic states. The energy difference between the contours is 200 keV for all plots. Note the different scales for the plots. Table II lists the configuration and deformation parameters associated with each minimum.

for the two-quasiparticle configurations but considering only four quasi-neutron, or 2 quasi-neutron, and 2 quasi-proton, configurations. The levels are listed in order of increasing energy, and the lowest predicted state ($J^\pi = 12^+$ at 4.48 MeV) contains all three of the quasi neutrons, which were discussed in the previous section in terms of forming the $J^\pi = 5^-$ and 8^- states. This $7/2^-[523] \otimes 7/2^+[404] \otimes 9/2^-[514] \otimes 1/2^+[400]$ configuration is calculated to have $|\gamma| = 30°$. Since this is triaxial, the blocked states are not pure Nilsson orbitals, and the minimum in the plot does not represent a pure $K^\pi = 12^+$ state. The theoretical assignment of $K^\pi = 12^+$ is

TABLE IV. Measured hindrances for transitions depopulating the $K^\pi = 8^-$ level.

J^π	K^π	E_{level} (MeV)	$t_{1/2}$ (ns)	E_γ (keV)	Mult.	Intensity	α [31]	Decay to	ΔK	ν	F_W	f_ν
8^-	8^-	2.786	73±3	286.5	$E2$	21(1)	0.0485	$K^\pi = 5^-$	3	1	16	16
				274.4	$E1$	0.08(4)	0.0131	ground state	8	7	$2.5\ 10^9$	22(2)
				204.0	if $E2$	12(1)	0.1468	$K^\pi = 5^-$	3	1	5.2	5.2
				204.0	if $M1$	12(1)	0.1133		3	2	$8.3\ 10^4$	288

become less deformed, and a typical Nilsson diagram for the $N = 74$ region shows that the energy difference between the $7/2^+[404]$ and $9/2^-[514]$ quasi-neutron orbits increases as the deformation decreases. Hence the excitation energy of the isomeric state increases as the deformation decreases, as shown in Fig. 10. This figure also shows that it is only in ^{128}Xe that the excitation energy of the $J^\pi = 7^-$ member of the $K^\pi = 5^-$ band is lower than that of the $K^\pi = 8^-$ state. Therefore in ^{128}Xe the $K^\pi = 8^-$ isomeric state preferentially decays to the $J^\pi = 7^-$ state, rather than by a seven-times K-forbidden $E1$ transition to the 8^+ member of the yrast band (assumed to have $K = 0$). The hindrance factors, F_W for the decay of the $K^\pi = 8^-$ isomeric state are given in Table IV. F_W is defined as

$$F_W = \frac{t_{1/2}^\gamma \binom{M}{E}\lambda}{t_{1/2}^W \binom{M}{E}\lambda}, \qquad (2)$$

where $t_{1/2}^\gamma \binom{M}{E}\lambda$ and $t_{1/2}^W \binom{M}{E}\lambda$ are the measured partial γ-ray half-life and the Weisskopf single-particle estimate, respectively. For K-forbidden transitions it is sometimes useful to compare Weisskopf hindrance factors, F_W, for different ΔK values [30]. The degree of K forbiddenness, ν, is defined by
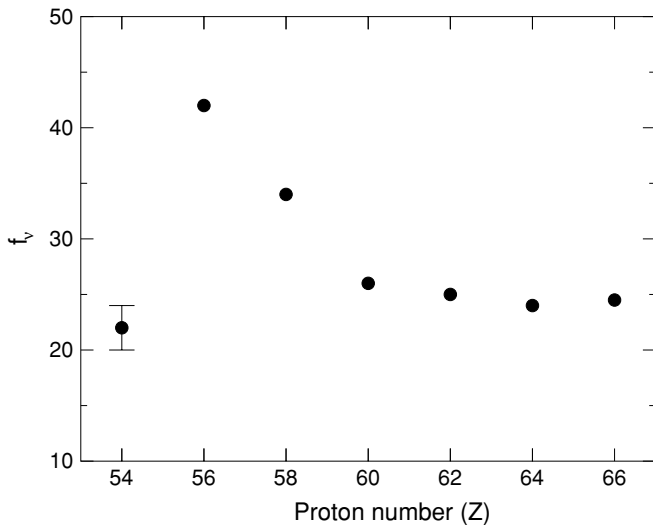
$$\nu = \Delta K - \lambda, \qquad (3)$$

and the hindrance per degree of K forbiddenness is defined by

$$f_\nu = (F_W)^{1/\nu}. \qquad (4)$$

In calculating the values of f_ν quoted in Table IV, it is assumed that the 6^- and 7^- states (at 2500 and 2582 keV, respectively) are members of the $K^\pi = 5^-$ band.

Figure 11 shows the f_ν value measured for the transition from the $K^\pi = 8^-$ state to the 8^+ member of the yrast band in comparison with those for other $N = 74$ isotones. The plot includes the recently measured value for ^{132}Ce [32]. The data point for ^{128}Xe indicates a big decrease in the f_ν value between ^{130}Ba and ^{128}Xe. Indeed, the ^{128}Xe value is surprisingly similar to those of the heavier ($Z \geqslant 60$) nuclei, which have well-deformed prolate shapes, and the K-selection rule would be expected to be correspondingly more rigorous.

There are two possible explanations for this. The first is in terms of the change in shape between ^{128}Xe and ^{130}Ba. Although the β deformation of all four relevant states is calculated to be about 0.16, the γ deformations are markedly different, with $|\gamma| = 6°$ and $|\gamma| = 32°$, respectively, for the isomeric and ground states in ^{128}Xe (see Table II), and $|\gamma| = 6°$ and $|\gamma| = 16°$ for ^{130}Ba [21]. Thus, while the isomeric states are both calculated to have $|\gamma| = 6°$, the ground states change from $|\gamma| = 32°$ for ^{128}Xe to $|\gamma| = 16°$ for ^{130}Ba. This is illustrated in Fig. 1 of Ref. [21]. The larger value of $|\gamma|$ for the ground state of ^{128}Xe as compared with ^{130}Ba implies more K mixing and hence a lower value of f_ν.

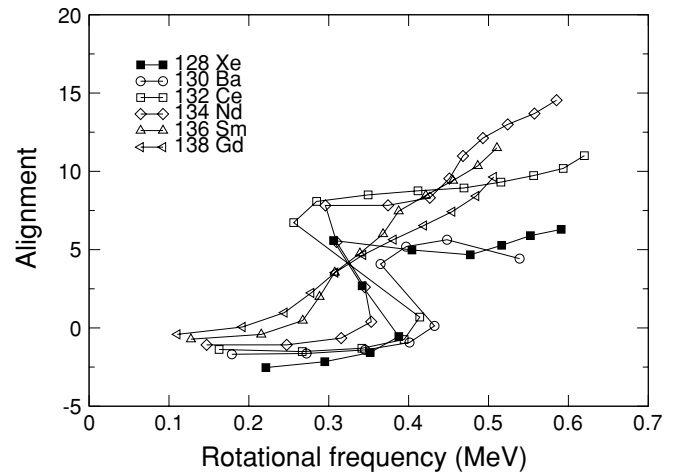FIG. 11. f_ν values for the transition from the $K^\pi = 8^-$ state to the 8^+ member of the yrast band in the $N = 74$ isotones.

FIG. 12. Experimental alignments for ^{128}Xe, ^{130}Ba, ^{132}Ce, ^{134}Nd, ^{136}Sm and ^{138}Gd. Harris reference parameters of $\mathcal{I}_0 = 17.0\hbar^2$ MeV^{-1} and $\mathcal{I}_1 = 25.0\hbar^4$ MeV^{-3} have been used for all nuclei.
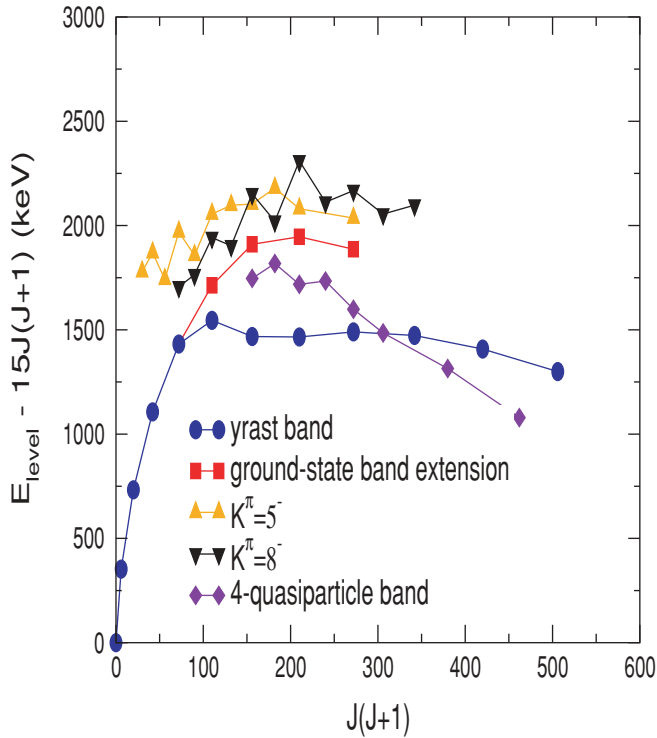
FIG. 13. (Color online) Excitation energy minus an arbitrary reference rotor plotted against $J(J+1)$ for the yrast band (circles), the ground-state band extension (squares), bands built on the $K^\pi = 5^-$ (triangles up) and $K^\pi = 8^-$ (triangles down) intrinsic states and the proposed four-quasiparticle band (diamonds).

The second explanation follows the discussion in Ref. [9], where the differences in f_ν are interpreted in terms of the amount of mixing in the yrast 8^+ state to which the $K^\pi = 8^-$ state decays. This interpretation is linked to the alignment in the yrast band, and Fig. 12 shows this property for the relevant $N = 74$ nuclei. The figure shows that the backbend for ^{128}Xe starts to occur around $J^\pi = 8^+$, which implies that there is considerable K mixing in the $J^\pi = 8^+$ state. Hence the decay from the $J^\pi = K^\pi = 8^-$ state will not be as hindered as might otherwise be expected. The ^{130}Ba and ^{132}Ce backbends begin $2\hbar$ higher, but it is of note that the alignment for ^{128}Xe is very similar to that for ^{134}Nd, and, indeed, the f_ν value is also very similar. Note also, however, that the existence of an isomeric state in ^{128}Xe does imply that K is in some sense conserved in its decay. The transition to the yrast band in this case is hindered by a factor of 2.5×10^9, compared with typical allowed hindrances of about 10^4.

D. Rotational behavior

The band built on the $J^\pi = 10^+$ state at 3364 keV is most likely the extension of the ground-state band with the previously observed yrast states corresponding to the $(\pi h_{11/2})^2$ quasi-proton configuration suggested by Wyss *et al.* [1]. Analogous positive-parity s bands have been discussed in the

neighboring Xe, Ba, and Ce nuclei, but the lack of experimental data on the extension of the ground-state band prevented Wyss *et al.* from making similar conclusions in ^{128}Xe.

A plot of excitation energy against $J(J+1)$ for the ground-state, $K^\pi = 5^-$ and 8^-, and four-quasiparticle bands is shown in Fig. 13. The figure shows that the yrast band begins to follow a rotational pattern at $10\hbar$. In the case of the band built on the $K^\pi = 5^-$ intrinsic state, Fig. 13 shows a very marked odd-even staggering, with the odd-spin levels being pushed lower in energy at the bottom of the band and the reverse being true above the 11^- state. This is perhaps not surprising, however, given that the PES calculations predict a γ deformation for this structure of $|\gamma| = 35.4°$, and Fig. 8 indicates that the nucleus is very γ soft.

The behavior of the $K^\pi = 8^-$ band is similarly complex, with Fig. 13 showing odd-even staggering with the even-spin levels pushed up in energy. Consistent with this, the branching ratios of the $\Delta J = 1$ and $\Delta J = 2$ transitions in this band are not observed to follow a simple rotational model.

V. CONCLUSIONS

An extended decay scheme for ^{128}Xe has been established in the current work with the yrast band being extended to $22\hbar$. Signature partner bands built on the $K^\pi = 5^-$ and $K^\pi = 8^-$ intrinsic states have been shown to exhibit strong odd-even staggering in their level energies. A $9/2^-[514] \otimes 1/2^+[400]$ two-quasiparticle configuration is proposed for the $K^\pi = 5^-$ configuration. A half-life of 73(3) ns has been measured for the $K^\pi = 8^-$ intrinsic state, which has a $9/2^-[514] \otimes 7/2^+[404]$ two-neutron configuration. A possible four-quasiparticle state has been observed at 4087 keV.

The configuration-constrained blocking method has been used to calculate potential energy surfaces and excitation energies for the ground and intrinsic states. The results predict triaxial shapes for the ground state and the $K^\pi = 5^-$ intrinsic state and a nearly axially symmetric shape for the $K^\pi = 8^-$ isomeric state. The decay from this latter state to the yrast band has a reduced hindrance per degree of forbiddenness of 22(2), which is much lower than for the neighbouring $N = 74$ nucleus ^{130}Ba. This reduction is considered to be at least partly due to K mixing in the 8^+ yrast state to which the isomer decays.

[1] R. Wyss, A. Granderath, R. Bengtsson, P. von Brentano, A. Dewald, A. Gelberg, A. Gizon, J. Gizon, S. Harissopulos, A. Johnson, W. Lieberz, W. Nazarewicz, J. Nyberg, and K. Schiffer, Nucl. Phys. **A505**, 337 (1989).

[2] R. F. Casten and P. von Brentano, Phys. Lett. **B152**, 22 (1985).

[3] U. Neuneyer, A. Mertens, R. Kuhn, I. Wiedenhover, O. Vogel, M. Wilhelm, M. Luig, K. O. Zell, A. Gelberg, P. von Brentano, and T. Otsuka, Nucl. Phys. **A607**, 299 (1996).

[4] L. Goettig, Ch. Droste, A. Dygo, T. Morek, J. Srebrny, R. Broda, J. Styczen, J. Hattula, H. Helppi, and M. Jaaskelainen, Nucl. Phys. **A357**, 109 (1981).

[5] H. F. Brinckmann, C. Heiser, K. F. Alexander, W. Neubert, and H. Rotter, Nucl. Phys. **A81**, 233 (1966).

[6] D. Ward, R. M. Diamond, and F. S. Stephens, Nucl. Phys. **A117**, 309 (1968).

[7] D. G. Parkinson, I. A. Fraser, J. L. Lisle, and J. C. Willmott, Nucl. Phys. **A194**, 443 (1972).

[8] A. M. Bruce, P. M. Walker, P. H. Regan, G. D. Dracoulis, A. P. Byrne, T. Kibédi, G. J. Lane, and K. C. Yeung, Phys. Rev. C **50**, 480 (1994).

[9] A. M. Bruce, A. P. Byrne, G. D. Dracoulis, W. Gelletly, T. Kibédi, F. G. Kondev, C. S. Purry, P. H. Regan, C. Thwaites, and P. M. Walker, Phys. Rev. C **55**, 620 (1997).

[10] W. Krolas, R. Grzywacz, K. P. Rykaczewski, J. C. Batchelder, C. R. Bingham, C. J. Gross, D. Fong, J. H. Hamilton, D. J. Hartley, J. K. Hwang, Y. Larochelle, T. A. Lewis, K. H. Maier, J. W. McConnell, A. Piechaczek, A. V. Ramayya, K. Rykaczewski, D. Shapira, M. N. Tantawy, J. A. Winger, C.-H. Yu, E. F. Zganjar, A. T. Kruppa, W. Nazarewicz, and T. Vertse, Phys. Rev. C **65**, 031303(R) (2002).

[11] D. M. Cullen, M. P. Carpenter, C. N. Davids, A. M. Fletcher, S. J. Freeman, R. V. F. Janssens, F. G. Kondev, C. J. Lister, L. K. Pattison, D. Seweryniak, J. F. Smith, A. M. Bruce, K. Abu Saleem, I. Ahmad, A. Heinz, T. L. Khoo, E. F. Moore, G. Mukherjee, C. Wheldon, and A. Woehr, Phys. Lett. **B529**, 42 (2002).

[12] K. Miyano, Nuclear Data Sheets **69**, 429 (1993).

[13] F. R. Xu, P. M. Walker, J. A. Sheikh, and R. Wyss, Phys. Lett. **B435**, 257 (1998).

[14] G. D. Dracoulis and A. P. Byrne, ANU-P/1052, 115 (1995) (unpublished).

[15] C. Pearson, Sort-shell sort-code (private communication).

[16] D. C. Radford, Nucl. Instrum. Methods Phys. A **361**, 297 (1995).

[17] W. Urban, ANA softwarem, Physics Department University of Manchester, U. K. (1994).

[18] K. S. Krane, R. M. Steffen, and R. M. Wheeler, Nucl. Data Tables **11**, 351 (1973).

[19] T. Lönnroth, S. Vadja, O. C. Kistner, and M. H. Rafailovich, Z. Phys. A **317**, 215 (1984).

[20] R. Reinhardt, A. Dewald, A. Gelberg, W. Lieberz, K. Schiffer, K. P. Schmittgen, K. O. Zell, and P. von Brentano, Z. Phys. A **329**, 507 (1988).

[21] F. R. Xu, P. M. Walker, and R. Wyss, Phys. Rev. C **59**, 731 (1999).

[22] T. Lönnroth, Z. Phys. A **315**, 183 (1984).

[23] F. Seiffert, W. Lieberz, A. Dewald, S. Freund, A. Gelberg, A. Granderath, D. Lieberz, R. Wirowski, and P. von Brentano, Nucl. Phys. **A554**, 287 (1993).

[24] O. Vogel, A. Dewald, P. von Brentano, J. Gableske, R. Krücken, N. Nicolay, A. Gelberg, P. Petkov, A. Gizon, J. Gizon, D. Bazzacco, C. Rossi Alvarez, S. Lunardi, P. Pavan, D. R. Napoli, S. Frauendorf, and F. Dönau, Phys. Rev. C **56**, 1338 (1997).

[25] O. Zeidan, D. J. Hartley, L. L. Riedinger, M. Danchev, W. Reviol, W. D. Weintraub, Jing-ye Zhang, A. Galindo-Uribarri, C. J. Gross, S. D. Paul, C. Baktash, M. Lipoglavsek, D. C. Radford, C. H. Yu, D. G. Sarantites, M. Devlin, M. P. Carpenter, R. V. F. Janssens, D. Seweryniak, and E. Padilla, Phys. Rev. C **65**, 024303 (2002).

[26] G. D. Dracoulis, C. Fahlander, and M. P. Fewell, Nucl. Phys. **A383**, 119 (1982).

[27] F. G. Kondev, R. V. F. Janssens, M. P. Carpenter, K. Abu Saleem, I. Ahmad, M. Alcorta, H. Amro, P. Bhattacharyya, L. T. Brown, J. Caggiano, C. N. Davids, S. M. Fischer, A. Heinz, B. Herskind, R. A. Kaye, T. L. Khoo, T. Lauritsen, C. J. Lister, W. C. Ma, R. Nouicer, J. Ressler, W. Reviol, L. L. Riedinger, D. G. Sarantites, D. Seweryniak, S. Siem, A. A. Sonzogni, J. Uusitalo, P. G. Varmette, and I. Wiedenhöver *et al.*, Phys. Rev. C **62**, 044305 (2000).

[28] M. Nomura, Phys. Lett. **B55**, 357 (1975).

[29] P. D. Cottle, K. A. Stuckey, and K. W. Kemper, Phys. Lett. **B219**, 27 (1989).

[30] K. E. G. Löbner, *The Electromagnetic Interaction in Nuclear Spectroscopy,* edited by W. D. Hamilton (North Holland, Amsterdam, 1975), p. 141.

[31] T. Kibédi, T. W. Burrows, M. B. Trzhaskovskaya, and C. W. Nestor Jr., AIP Conf. Proc. **769**, 268 (2005).

[32] T. Morek, J. Srebrny, Ch. Droste, M. Kowalczyk, T. Rzcca-Urban, K. Starosta, W. Urban, R. Kaczarowski, E. Ruchowska, M. Kisieliński, A. Kordyasz, J. Kownacki, M. Palacz, E. Wesolowski, W. Gast, R. M. Lieder, P. Bednarczyk, J. Meczyński, and J. Styczeń, Phys. Rev. C **63**, 034302 (2001).